Can second order nonlinear spectroscopies selectively probe optically "dark" surface states in small semiconductor nanocrystals?

Anne Myers Kelley

Chemistry & Chemical Biology, University of California, Merced

5300 North Lake Rd., Merced, CA 95343

amkelley@ucmerced.edu

Abstract

Second order nonlinear responses such as sum frequency and second harmonic generation arise from the response of a material system to the second power of an incident electromagnetic field through the material's first hyperpolarizability or second-order optical susceptibility. These quantities are nonzero only for noncentrosymmetric systems, but different length scales of the noncentrosymmetry give rise to second harmonic or sum frequency radiation with different spatial and coherence characteristics. This Perspective discusses the possible contributions to the second-order signal from films of small semiconductor quantum dots and addresses whether such experiments are expected to selectively enhance transitions to surface defects or trap states in such systems. It points out how "surface" and "bulk" contributions to the sum frequency or second harmonic signal should be distinguishable through their angular dependence in a scattering geometry. It also explores possible mechanisms whereby second order spectroscopies might provide access to surface states that are very weak or absent in other forms of optical spectroscopy.

I. Introduction

Second-order nonlinear optical processes such as sum frequency generation (SFG) and second harmonic generation (SHG) are allowed in a material (within the electric dipole approximation for the radiation-matter interaction) only if the material lacks a center of symmetry.[1] This property has been exploited to develop SHG and SFG as specific probes of surfaces and interfaces, as the reduction of symmetry at the interface between two centrosymmetric media results in signal being generated only from the region near the interface. SHG and SFG are now well-established techniques for probing the structures of surfaces and interfaces, studying chemical reactions occurring at surfaces, and detecting small quantities of analytes adsorbed to surfaces.[2] Figure 1 diagrams the "doubly resonant" versions of SHG as well as two forms of SFG, the more common infrared-visible type that accesses vibrational resonances and the visible-visible type more suitable for probing electronic resonances.

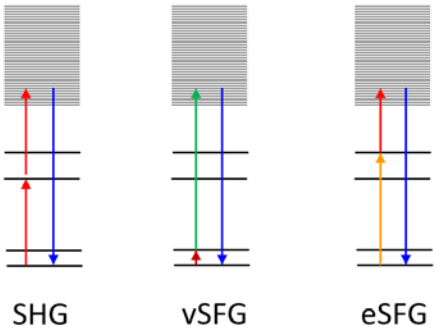

Figure 1. Doubly resonant second harmonic generation (SHG), vibrational sum frequency generation (vSFG), and electronic sum frequency generation (eSFG).

The original experiments in surface second harmonic generation involved interfaces that were essentially planar relative to the spot size of the exciting laser. Objects such as biological cells, micelles, polymer microspheres, and metal or semiconductor nanocrystals also have surfaces, but the surfaces are highly curved and in a typical experiment many such particles are irradiated by the exciting beams. Consider a polystyrene sphere suspended in water. If the interacting entity is considered to be the entire sphere, then it is centrosymmetric and should not have a second-order optical response. However, if considered as a set of curved surfaces, each part of the polystyrene/water interface is locally noncentrosymmetric and should generate

a second-order signal. Eisenthal and co-workers showed that if the particle is small compared with the wavelength of the light, the contributions to the nonlinear polarization from opposite surfaces cancel each other and result in no net second harmonic generation, while if the sphere is not small compared to the wavelength this cancellation is incomplete and a nonzero second harmonic signal is expected.[3] They and other groups have since expanded on this treatment both theoretically and experimentally, showing that the intensity of the second harmonic produced falls off rapidly with decreasing particle size.[4-7] Dadap and co-workers[5] showed that the second-harmonic intensity should scale as the sixth power of the radius of the spherical particle, and estimated that surface scattering from particles with radii as small as 5-10 nm should be detectable. In addition, the wavevector of the generated second harmonic light varies from nearly colinear with that of the exciting light for large particles to nearly perpendicular to it for the smallest particles.[7-11]

Many of the experiments designed to probe second-order processes at the surfaces of micron- or nanometer-sized particles are carried out in liquid suspensions, and care is taken to insure that no signal is collected from macroscopic interfaces such as between the liquid and the wall of the sample cell. In this case the second-order signal must originate entirely from either the surfaces of the particles ("surface" contribution) or, if they have a noncentrosymmetric internal structure or overall shape, from the particle as a whole ("bulk" contribution). Many other second-order nonlinear optical experiments are carried out on nanoparticles deposited as a film on a substrate. In this case the nonlinear signal may arise from the mechanisms described above and/or from any additional nonlinearity induced by the bulk film-air or film-substrate interfaces. Two recent studies suggest that sum frequency spectroscopy in solid films of semiconductor nanocrystals can selectively probe trap states at the nanocrystal surface,[12-13] even if these states are essentially "dark" to other forms of spectroscopy. This Perspective addresses

both the surface selectivity of experiments performed in this geometry and the selection rules that should apply. It also proposes experiments that could help clarify these issues.

II. Second-order nonlinear optical responses—noncentrosymmetry, length scales, and coherence

An electromagnetic field $\vec{E}$ interacting with a molecule or atom induces a dipole $\vec{p}$ given by

$$\vec{p} = \alpha : \vec{E} + \frac{1}{2}\beta : \vec{E}\vec{E} + \frac{1}{6}\gamma : \vec{E}\vec{E}\vec{E} + \cdots \quad (1)$$

where α is the linear polarizability, β is the first hyperpolarizability, and γ is the second hyperpolarizability. The quantities α, β, and γ are first, second, and third rank tensors, respectively, but the tensorial nature of these quantities is not explicitly treated here. The term quadratic in $\vec{E}$ (proportional to β) is the focus of this Perspective. It is assumed that $\vec{E}$ can be written as a superposition of plane waves having frequency ω and wavevector $\vec{k}$. If the incident field consists of a single frequency, the induced polarization can have components oscillating at 2ω which produce radiation at the second harmonic frequency. If the incident field consists of two different frequencies ω_1 and ω_2, the induced polarization can have components oscillating at $\omega_1+\omega_2$ which produce radiation at the sum frequency. Sum frequency or second harmonic radiation can be produced only if β, which in general is a function of both frequency and the polarization indices, is nonzero. β is a property of the atom or molecule and can be nonzero only if the atom or molecule does not have a center of symmetry. This can be rationalized by recognizing that if the molecule has a center of symmetry, the polarization induced by applying an electric field along $+\vec{r}$ must be equal and opposite to that induced by applying a field of equivalent strength along $-\vec{r}$. But the electric field is an odd function of position, so only odd terms in the expansion of Eq. (1) can be nonzero for centrosymmetric systems.

Eq. (1) refers to the interaction of one molecule or atom with an electromagnetic field. In most experiments the detected radiation results from summing the electromagnetic fields produced by the polarizations of a large number of molecules in the sample. In most gases, liquids, or fluid solutions, the positions and orientations of different molecules are random and essentially uncorrelated and there is no net coherence between the fields generated by the different molecules. The detected signal intensity is simply the sum of the intensities generated by each molecule, *e.g.* for second harmonic,

$$I_{HRS}(2\omega) \sim N\left|\beta : \vec{E}\vec{E}\right|^2 \qquad (2)$$

where the subscript *HRS* refers to hyper-Rayleigh scattering, the usual term for incoherent second harmonic scattering from a random arrangement of scatterers, and N is the concentration. The polarization properties of the scattered light are determined by the tensorial nature of β and the polarizations of the incident fields. The angular distribution of the scattered wavevectors is that characteristic of dipolar radiation with those polarization properties. Note that the usual analysis of hyper-Rayleigh scattering assumes not only that the scatterers are randomly positioned and oriented, but also that the fluctuations in their positions and orientations are fast on the time scale of the measurement such that all possible arrangements are averaged. When the scatterers are randomly distributed but not fluctuating, *e.g.* for nonlinear chromophores immobilized in a polymer matrix, this temporal averaging is incomplete and the hyper-Rayleigh intensity detected in a particular direction will vary as the sample is translated through the excitation beam, sampling different arrangements of chromophores.[14]

If the individual entities interacting with the incident field are not randomly arranged on a length scale over which the field varies, then their arrangement has to be taken into account explicitly. The "macroscopic" version of eq. (1) is

$$\vec{P} = \chi^{(1)}:\vec{E} + \frac{1}{2}\chi^{(2)}:\vec{E}\vec{E} + \frac{1}{6}\chi^{(3)}:\vec{E}\vec{E}\vec{E} + \cdots \quad (3)$$

where $\vec{P}$ is the macroscopic bulk polarization and $\chi^{(n)}$ is the n^{th} order optical susceptibility, which again is an n^{th} rank tensor and generally depends on frequency. $\chi^{(2)}$ is the relevant susceptibility for second order processes and its relationship to the constituent β values depends on the positions and orientations of the individual atoms or molecules. The same symmetry properties hold as for Eq. (1): if the bulk macroscopic system is net centrosymmetric, then no coherent second order radiation can be produced. For example, noncentrosymmetric molecules may form a centrosymmetric crystal that will have a zero bulk $\chi^{(2)}$. A collection of noncentrosymmetric molecules randomly distributed in an isotropic liquid can produce hyper-Rayleigh scattering but not coherent second harmonic; β is nonzero but $\chi^{(2)}$ is zero.

More interesting are the intermediate cases where the material is isotropic on sufficiently long length scales but noncentrosymmetric on shorter scales. An excellent review by Roke and Gonella[15] summarizes the characteristics of nonlinear light generation from objects that are structured over a wide range of length scales. Objects smaller than ~10 nm in size (most molecules and small nanoparticles) exhibit primarily hyper-Rayleigh scattering (HRS), which can be viewed as radiation from a single point dipole on each object. As the object becomes large enough that the electromagnetic field is not constant across its dimensions, the fields generated at different positions on the object must be added to give the total response. For an object composed of an isotropic material β is nonzero only at the interface between the object and its surroundings, and if the interfaces are separated by some distance the contributions from the different interfaces do not cancel completely, resulting in what is usually referred to as second harmonic scattering (SHS) or sum frequency scattering (SFS). The signal produced from a randomly positioned and oriented ensemble of such objects is still incoherent but has an

angular distribution that is a strong function of the size and shape of the object.[4, 8-9, 15] Note that while HRS and SHS have theoretically different origins, they are both macroscopically incoherent with a distribution of wavevectors for the generated radiation, they are typically observed in similar experimental configurations, and they may be simultaneously present. Note also that the terminology of Roke and Gonella[15] used in this Perspective is not adopted consistently in the literature.

Much of the experimental work on SHS has utilized electronically resonant, highly nonlinear chromophores such as malachite green adsorbed to the surfaces of polymer spheres in solution. The second harmonic signal is measured as a function of chromophore concentration in order to determine the thermodynamics of binding of the chromophore to the surface. The concentration dependence is fit to a function of the type[16]

$$I = B + N_S\left|a + b\theta e^{i\varphi}\right|^2 \quad (4)$$

where B accounts for background hyper-Rayleigh scattering from unbound chromophores and/or the solvent, N_S is the concentration of particles, a gives the contribution to the nonlinear polarization from the bare particle itself, b is proportional to the nonlinear susceptibility of the dye molecules adsorbed to the surface, θ is the fractional surface coverage, and φ is the optical phase difference between the field produced by the nonlinear chromophores and the bare particle surface. The detected second harmonic intensity is linearly proportional to the concentration of particles and also to the concentration of unbound chromophores (through B) because the contributions from different particles or different free chromophores do not add coherently, but it depends quadratically on the number of bound chromophores per particle (through θ) because chromophores bound to the same particle add coherently to the signal. In many reported experiments of this type,[3-4, 6-8, 16-18] both B and a are found to be nearly negligible and the dominant source of signal is from the chromophores bound to the particles, in which

case the second harmonic intensity scales as $N_S|b\theta|^2$. In some experiments, however, the conditions are chosen such that both the hyper-Raman scattering from the free chromophores and the second harmonic scattering from the chromophores adsorbed to the particles are of comparable magnitude.[19]

Second harmonic scattering experiments carried out in the absence of any adsorbed dye have been interpreted to show both bulk and surface contributions to the nonlinear signal. Gold and silver nanoparticles with nominally centrosymmetric shapes and internal structures produce strong second harmonic scattering in solution that can be shown, through angle and polarization resolved measurements, to contain both dipolar and quadrupolar contributions.[20-26] The quadrupolar part is assigned to gradients of the electromagnetic field within the particle, which become negligible in the limit of sufficiently small particles. The dipolar contribution is often assigned to surface scattering, although it may also have contributions from asymmetry in the shape of the particle.

Second harmonic scattering from semiconductor quantum dots (QDs) including CdSe and CdS has also been studied.[27-34] The QDs were all in the size range (< 10 nm diameter) where hyper-Rayleigh scattering is expected to dominate and these experiments are most simply interpreted as symmetry-allowed HRS. Both of the common crystal structures (wurtzite and zincblende) are noncentrosymmetric and similar QDs have been found to have large ground-state dipole moments, confirming an asymmetric structure.[35-38] Several of these experiments have also been interpreted to show both bulk (HRS) and surface (SHS) contributions to the signal.[27-28, 31-32] In particular, Jacobsohn and Banin concluded that both bulk and surface effects are operative based on the dependence of the second harmonic intensity on QD size and on exchanging the native ligands for ligands with a large first hyperpolarizability. This interpretation may be complicated by the fact that small QDs are often highly faceted and not

truly spherical, and different facets may bind ligands differently, increasing the asymmetry of the overall structure.

Both hyper-Rayleigh scattering and second harmonic scattering from the surfaces of particles in liquid solution are well known and widely studied. There are far fewer reports of the analogous sum frequency processes ($\omega_1 + \omega_2$ where $\omega_1 \neq \omega_2$). There have been some reports of vibrational SFS, *e.g.* for lipids adsorbed to oil nanodroplets in water[39-40] and for aerosol particles.[41] I am not aware of any studies of the sum frequency analog of hyper-Rayleigh scattering from molecules or very small particles, but there is no reason why this process should not be detectable. Sum frequency generation has been observed from solutions of chiral chromophores near an electronic resonance, but in this case the sum frequency was generated as a coherent beam in the bulk phase-matched direction.[42] This was possible because, while the solution contained randomly positioned and oriented chromophores, the bulk liquid was noncentrosymmetric owing to the chirality of the chromophores.

When the interfacial region becomes large compared with the wavelength of the light, the second harmonic or sum frequency light is generated as a coherent beam in the macroscopically phase-matched direction, in either reflection or transmission geometry. This is usually referred to as second harmonic generation (SHG) or sum frequency generation (SFG). SHG and SFG from planar interfaces have been the subject of many reviews.[43-47] A wide variety of systems have been studied including the surfaces of liquids or solids with air or vacuum, with or without other species adsorbed to the interface, as well as buried liquid-liquid, liquid-solid, and solid-solid interfaces. The main characteristic of these processes is that because the interface is essentially planar over the entire spot size of the exciting laser(s), the contributions from all parts of the interface add coherently to produce a signal having a well-defined direction which is detected in either transmission or, more often, reflection. The constructive interference

between the nonlinear polarizations created at each point on the surface makes this technique quite sensitive to small interfacial areas or to small numbers of adsorbates at an interface. The surrounding bulk materials generally make an insignificant contribution to the signal if they are isotropic, although contributions to the bulk response from electric quadrupole and magnetic dipole terms in the radiation-matter interaction may in some cases be important.[47-48] The intensity of the second harmonic or sum frequency radiation is proportional to the square of the second-order nonlinear polarization which, as in eq. (3), is proportional to the second-order susceptibility, $\chi^{(2)}$. The relationship between $\chi^{(2)}$ and the properties of the species at the interface depends on the system. In general, $\chi^{(2)}$ is given by a sum of the first hyperpolarizabilities (β) of the species at the interface, scaled by appropriate geometric factors that depend on the polarizations of the fields and the orientations of the hyperpolarizability tensors relative to the surface. For a single contributing interfacial species, the susceptibility is proportional to the number density of adsorbed species and so the second harmonic or sum frequency signal intensity is proportional to the square of the adsorbed surface density, just as for SHS or SFS from adsorbates on the surfaces of particles.

III. Distinguishing surface from bulk contributions to nonlinear scattering

I now return to the situation of particles dispersed in a suspension that may have both bulk (HRS or its sum-frequency analog) and surface (SHS or SFS) contributions to the nonlinear polarization. As discussed above, these two processes may be present simultaneously and they both produce radiation that has no macroscopic coherence and no single, well-defined wavevector. However, in many cases these two forms of nonlinear light generation should be clearly separable through the angular distribution of wavevectors for the emitted light.[19]

In hyper-Rayleigh scattering the emission from each particle is that characteristic of a single dipole, and there is no coherence among different emitters because they are assumed to be randomly positioned and oriented. The depolarization ratio (the relative intensities of scattered radiation polarized perpendicular and parallel, respectively, to the excitation light polarization) is a well defined but complicated function of the components of the hyperpolarizability tensor.[49] The angular distribution of emitted wavevectors is determined purely by the polarization, independent of the wavevector for the incident light. For example, if the excitation light is polarized along the z direction and propagating along the x direction (here assuming second harmonic generation where both input fields are the same), all propagation directions for the hyper-Rayleigh scattered radiation in the xy plane are equally probable. The emission retains no "memory" of the wavevector of the excitation.

The situation is quite different with surface second harmonic scattering because the different parts of the surface emit with well defined relative phases and exhibit both constructive and destructive interferences which depend on both the size of the particle and the propagation direction of the incident light. The specific angular emission pattern also depends on the hyperpolarizability tensor for the surface-active species and its orientation relative to the surface normal and is different for each system, but in general the distribution of emitted wavevectors is not isotropic in the xy plane for z-polarized light.[4-5, 8-9, 15] The calculated emission patterns have been verified by comparison with experiment in systems for which the bulk contribution is expected to be negligibly weak.

For a system in which the importance of the surface contribution is not known, measurement of the angular dependence of the second harmonic or sum frequency signal can be used to estimate its importance.[19] Accurate calculation of the surface contribution requires knowledge of the components and orientation of the surface hyperpolarizability tensor as well

as the size and shape of the particle, none of which may be well defined for systems such as semiconductor nanocrystals with complicated mixtures of surface ligands and/or poorly characterized surface trap states. However, deviations of the angular distribution from that expected for dipolar emission may reasonably be attributed to the surface contributions.

IV. Combining length scales—macroscopic interfaces composed of nanoparticles

I now consider the case where particles, which may themselves have both bulk and surface contributions to their nonlinear optical response, are deposited as a solid film on a substrate (Figure 2). The contribution from the bulk response of the particles (HRS or its sum-frequency analog) will produce a dipolar emission pattern from each particle, while the contribution from the surface of the particles (SHS or SFS) will produce a more complicated angular dependence that depends on both the wavevector(s) and the polarization(s) of the incident beam(s), as well as the orientation of the hyperpolarizability tensor of each entity on the surface. There may also be additional contributions to the nonlinear response from the direct interaction between the

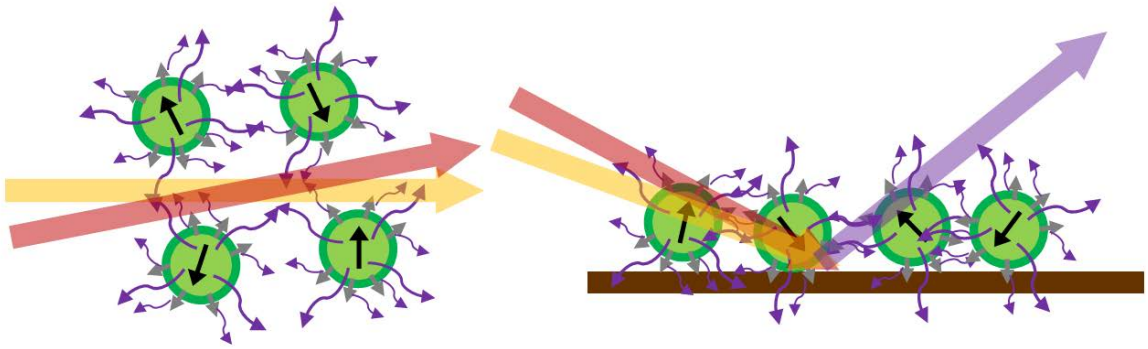

Figure 2. Cartoon of sum frequency generation (red plus yellow arrows to produce violet) from particles in solution (left) and on a substrate (right). The particles produce a bulk contribution to the nonlinear polarization (large black arrows) as well as a surface contribution (small gray arrows), both of which radiate the sum frequency (violet arrows). Randomly arranged particles in solution generate only incoherent sum frequency light (left), while particles on a surface generate a macroscopically coherent sum frequency beam (right).

surfaces of the particles and the substrate. In general, however, in all directions except the macroscopically phase-matched one the contributions from different particles will add incoherently as in the case of particles randomly distributed in a liquid, and the signal will be dominated by a coherent beam in the phase-matched direction. The coherent, phase-matched signal intensity should scale as the square of the density of particles on the surface. I have not found published studies in which the same particles were examined both in solution in a scattering geometry and deposited on a substrate. Roke's group measured sum frequency spectra from SDS surfactant adsorbed to both the surface of oil droplets in solution and the CaF_2-D_2O bulk interface, a different comparison, and presented a detailed discussion of the different phase-matching conditions for each case.[9] This group also measured sum frequency scattering from polymer microspheres deposited between CaF_2 windows, but stated that the samples were prepared with a sufficiently low surface coverage that only a few spheres were probed,[50] minimizing any coherent, phase-matched contribution to the signal.

Vibrational SFG has been widely used to study the properties of ligands on the surfaces of small nanoparticles including gold,[51-52] silver,[51] ceria,[53] and CdSe.[54-55] In all of these experiments the nanoparticles were deposited on a solid substrate and the sum-frequency radiation was detected in the phase-matched direction; refs. 52 and 53 state that the macroscopic asymmetry provided by the substrate is needed to detect the signal. In these studies, the vSFG technique necessarily probes ligands on the surface of the nanoparticle because that is the only place the ligands are. There is no distinction between surface and bulk contributions to the signal because the ligands whose resonances are probed reside exclusively on the surfaces of the particles. vSFG was also used to probe the CH stretches of surfactant encapsulated polyoxometalate ions adsorbed to the air-water interface in a reflection geometry.[56] Again, only

the vibrations of the surfactant were probed and the surfactant is on the outside of the structure, but there is no meaningful distinction between bulk and surface contributions.

V. Surface selectivity in nonlinear optical measurements of nanoparticles at bulk interfaces?

In the above applications of vibrational SFG to nanoparticles at bulk interfaces, it is clear from the vibrational resonances observed that the experiment is probing only the ligands on the surface of the nanoparticles. Several recent papers have argued that even when probing spectral regions of small semiconductor quantum dots where both the core and the surface of the nanoparticle may have contributing resonances, SFG or SHG spectroscopy should have some selectively for surface states.[12-13, 57] Ref. 57 applied SHG spectroscopy to small CdSe QDs with diameters of 2.3-2.4 nm. Features not clearly discernible in the absorption or photoluminescence excitation spectra were observed and assigned to previously identified excitonic transitions, and surface character was attributed to one of these features. While touting the surface selectivity of SHG, this paper does state that both the bulk and the surface are likely to contribute to the signals and the assignment of surface character was made based on the effect of oxidation on one spectral feature. Ref. 13 carried out IR-visible SFG on CdS QDs stated to be 20-40 nm in size. Resonances observed at visible wavelengths below the band-edge absorption were attributed to surface states. Ref. 12 applied electronic SFG (800 nm plus 500-750 nm) microspectroscopy to 4-7 nm CdSe QDs. The authors argued that eSFG should provide access to the usual one-photon and two-photon allowed transitions of the QD core as well as optically forbidden transitions involving both the core and the surface. Resonances were observed near wavelengths that correspond to known one- and two-photon allowed transitions of the QDs as well as at longer wavelengths that are not seen in the one- or two-photon excitation spectra, and these were assigned to surface states.

As discussed in Section III, surface and bulk contributions to the second-order nonlinear signal can be distinguished by their angular dependence when the experiments are performed in a scattering geometry (particles randomly dispersed in a liquid). This information is lost when the particles are deposited on a substrate and the signal is detected in the macroscopically phase-matched direction, as was the case in all of these experiments.

VI. Selection rules and observation of "dark" states

Refs. 12 and 13 both claim that sum frequency spectroscopy can probe surface states that are optically forbidden in other forms of spectroscopy. Surface states are known to have very low one-photon oscillator strengths, as evidenced by their almost negligibly weak absorption and weak, long-lived photoluminescence. The weak optical response is due to very small electron-hole overlap when either the electron or the hole is trapped, which should limit the cross-section in all optical spectroscopies. It is therefore hard to rationalize why these transitions should appear as strong one-photon resonances in the SFG spectrum. The long-wavelength resonances attributed to surface states in CdSe change somewhat after the samples are exposed to air, but so do features attributed to excitonic transitions of the CdSe core.[12, 57]

For a sum-frequency generation process that may include one-photon and/or two-photon resonances, the detected sum-frequency intensity is proportional to the absolute square of $\chi^{(2)}$, which can be expressed as[58]

$$\left|\chi^{(2)}\right|^2 \propto \left|\sum_n \sum_{n'} \left(\frac{1}{\omega_n - \omega_1 - i\Gamma_n} + \frac{1}{\omega_n - \omega_2 - i\Gamma_n}\right) \frac{\mu_{gn}\mu_{nn'}\mu_{n'g}}{\omega_{n'} - \omega_{sum} - i\Gamma_{n'}}\right|^2 \quad (5)$$

where ω_1 and ω_2 are the two input frequencies, $\omega_{sum} = \omega_1 + \omega_2$, ω_i is the frequency of state i, Γ_i is the homogeneous (dephasing) linewidth of state i, μ_{ij} is the transition dipole moment between states i and j, and the sums are over all potentially one-photon resonant (n) and two-

photon resonant (n') transitions. The corresponding one-photon absorption cross-section at frequency ω is given by

$$\sigma_{1PA} \propto \sum_n \frac{\Gamma_n |\mu_{gn}|^2}{(\omega_n - \omega)^2 + \Gamma_n^2} \quad (6)$$

and the two-photon absorption cross-section is (see ref. 59)

$$\sigma_{2PA} \propto \sum_{n'} \frac{\Gamma_{n'}}{(\omega_{n'} - \omega_{sum})^2 + \Gamma_{n'}^2} \left| \sum_n \mu_{gn} \mu_{nn'} \left(\frac{1}{\omega_n - \omega_1 - i\Gamma_n} + \frac{1}{\omega_n - \omega_2 - i\Gamma_n} \right) \right|^2 \quad (7)$$

The sums include, in principle, all vibrational and electronic (vibronic) transitions. Inhomogeneous broadening, which makes a large contribution to the widths of electronic transitions in most quantum dots, is not included in these expressions. The denominators in eq. (5) show that a maximum in the sum frequency signal is expected when one of the incident frequencies or the sum frequency is resonant with a transition from the ground state to a vibrationally or electronically excited state, as long as the transition dipole moment for that transition is nonzero. That is the same condition for the transition to be observed as a resonance in the absorption spectrum. However, a $g \rightarrow n$ transition that is strong in absorption may be absent in SFG if there are no states n' near the sum frequency for which $\mu_{nn'}$ and $\mu_{n'g}$ are both nonzero. In a centrosymmetric system, all states have either even or odd parity and the transition dipole operator connects only states with opposite parity. Therefore it is not possible for μ_{gn}, $\mu_{nn'}$ and $\mu_{n'g}$ to all be simultaneously nonzero, and there is no sum frequency signal from centrosymmetric systems.

The experiments of ref. 13 mix an IR wavelength between 5000 and 2800 nm (2000 to 3571 cm^{-1}) with a visible wavelength between 580 and 650 nm. All of these wavelengths are below the electronic band gap of the CdS nanocrystals; the IR wavelengths may be resonant with vibrations of the ligands, but it is not stated what the ligands are. Ref. 13 seems to imply (see Fig. 4 of that paper) that the vibrational resonances are unimportant and that only two-photon

electronic resonances (the states n' in Eq. 5) need to be considered. Fig. 5 of ref. 13 shows the SFG intensity as a function of the two-photon (sum frequency) wavelength, apparently obtained by fixing the IR wavelength and scanning the visible wavelength. Strong features are observed at two-photon energies that are well below the absorption onset but roughly correspond to observed trap state emission, which has a long lifetime corresponding to a weak one-photon oscillator strength. The two-photon absorption spectrum of CdS QDs has been reported,[60] but apparently only in the region near or above the band gap. Therefore it is not known whether the features observed in the 585-630 nm range of the SFG spectrum correspond to known two-photon states. What is surprising is that essentially no SFG intensity is observed with two-photon excitation in the region near the absorption onset (450-520 nm for these large QDs), given that the lowest-energy peak in the two-photon absorption spectrum of smaller CdS QDs is only slightly blue-shifted from the lowest one-photon absorption feature.[60]

Ref. 12 presents visible-visible sum frequency spectra for three different sizes of CdSe QDs, mixing 800 nm light with a visible continuum in the 500-750 nm range to produce signal in the 308-388 nm range. The 800 nm is below the band gap while the shorter-wavelength range of the continuum falls within the one-photon absorption of these QDs, so both one-photon and two-photon resonances (n and n' in Eq. 5) may contribute to the peaks in the plots of sum frequency intensity as a function of visible wavelength. However, given the high density of states at 300-400 nm there is unlikely to be sharp structure in the two-photon absorption spectrum at these energies, and the authors attribute the features in their SFG spectrum entirely to one-photon resonances with the visible continuum. Resonances close to peaks in the one-photon absorption spectra are indeed observed, but they are not the strongest peaks in the spectra. Some of the other peaks in the 500-650 nm range are attributed to previously assigned transitions that are mainly two-photon allowed,[12, 59, 61] but since there is no two-photon path to these states in the

experiment, it is not clear why their two-photon allowed character should cause them to appear. The strong resonances observed at longer wavelengths have no corresponding feature in the one- or two-photon absorption/excitation spectra and are attributed to surface states.[12]

One possible rationalization for the observation of relatively strong signals from surface trap states is that the excitonic states localized in the interior of the QD are approximately eigenstates of parity. Then only the odd-parity states would be one-photon allowed and only even-parity states two-photon allowed, and neither state could appear as a resonance in SFG. Surface trap states would not obey these symmetry selection rules and could possibly dominate the SFG spectrum even though they make negligible contributions to the one-photon and two-photon absorption spectra. However, as mentioned above, the observation of large ground-state dipole moments for most semiconductor quantum dots strongly suggests that these are not centrosymmetric structures with parity-forbidden transitions.

It has been pointed out that electronic SFG can reveal transitions that are nominally symmetry-forbidden.[62] However, this simply refers to the fact that in sufficiently symmetric structures, transitions that are electric dipole forbidden by symmetry at the ground-state equilibrium geometry may become allowed through excitation of a phonon that breaks the symmetry (vibronic coupling). The same mechanisms are operative in ordinary one-photon and two-photon absorption and are not special to SFG; the states n and n' in eqs. (5)-(7) are vibronic states, not purely electronic. Vibronic coupling does not explain why resonances not observed in one- or two-photon absorption appear in SFG. The strong excitonic transitions of CdSe and CdS QDs (*e.g.* $1S_{3/2}$-$1S_e$) have high oscillator strengths inconsistent with symmetry-forbidden, vibronically-induced transitions.

There is one other important difference between one- or two-photon absorption spectroscopy and second harmonic or sum frequency spectroscopy from the standpoint of

observing resonances. In an absorption process the linewidth of the final state, which generally has contributions from both inhomogeneous broadening and pure dephasing, does not influence the transition probability—each transition (n in eq. 6 and n′ in eq. 7) is a normalized Lorentzian. Increasing the linewidth of the final state transition does not change the integrated one-photon or two-photon absorption cross-section, but merely spreads it out over a broader frequency range. In contrast, in SHG or SFG these states are intermediate states in a three-photon process, and increasing the dephasing rate of an intermediate state (n in eq. 5) reduces the overall probability of the process, as does increasing the dephasing rate of an intermediate state in a two-photon absorption process (n in eq. 7). In SFG the contributions from different resonant states (*n* or *n′* in eq. 5) add at the level of the complex amplitude before being squared, potentially generating either constructive or destructive interferences when the resonant states are closely spaced in energy. This is similar to the effect of the excited-state linewidth on the resonance Raman excitation profile; increasing the homogeneous linewidth of the resonant state merely broadens the absorption spectrum, but both broadens and weakens the Raman excitation profile.[63-65] Reduction of the resonance Raman cross-section by interference effects among multiple intermediate states is also well established in resonance Raman spectroscopy of semiconductor QDs.[66] Little or nothing is known about the dephasing rates for trap state transitions in semiconductor QDs, but these effects may allow surface trap states to make a much larger contribution to intermediate resonances in SFG then would be expected based on their very low oscillator strengths. This was hinted at in ref. 12 and remains an interesting possibility for further exploration.

Finally, while the emphasis of this Perspective is second-order nonlinear spectroscopies, higher-order "multidimensional" pump-probe techniques have also been shown to access states that are too weakly allowed to be observed in linear spectroscopies including parity-forbidden

and spatially indirect excitons in semiconductor quantum wells,[67] sub-bandgap defect states in perovskites,[68] and surface states in GaAs.[69] In particular, the two-dimensional fourth-order analog of electronic sum frequency spectroscopy (2D-ESFG) revealed sub-bandgap surface states in bulk GaAs crystals that could not be observed in ordinary one-dimensional ESFG spectra.[69]

VII. Conclusions

Small semiconductor nanocrystals such as CdSe and CdS are known to have a noncentrosymmetric crystal structure and have been found to have large ground-state dipole moments. As such, they should generate second harmonic or sum frequency radiation without consideration of any surface effects. There may be additional contributions from the surface, and it should be possible to distinguish surface from bulk contributions by examining the angular dependence of the second harmonic or sum frequency emission in a scattering geometry (particles randomly dispersed in a liquid).

The observation of transitions to surface states as one-photon or two-photon resonances in sum frequency or second harmonic spectroscopy requires the same transition dipole matrix element(s) as for one- or two-photon absorption and should not be observable for truly "dark" states. However, transitions that are weakly allowed in absorption might make relatively large contributions to SHG or SFG if there are no resonant states that are simultaneously strongly one-photon and two-photon allowed. -In addition, trap states located below the band gap could produce unexpectedly strong resonances in SHG or SFG if they have very long dephasing times (small homogeneous linewidths) or fewer nearby transitions that can interfere destructively with their contributions to the nonlinear susceptibility. Definitive assignment of sum frequency

resonances to surface states must await experiments that synthetically modify the QD surfaces in well-defined ways to passivate or introduce trap states.

VIII. Acknowledgements

This work was supported by NSF grant CHE-1506803. I thank Prof. David F. Kelley for helpful comments.

References

1. Y. R. Shen, *The Principles of Nonlinear Optics*; John Wiley & Sons: New York, 1984.

2. R. M. Corn, D. A. Higgins, "Optical Second Harmonic Generation as a Probe of Surface Chemistry", Chem. Rev. **94**, 107 (1994).

3. H. Wang, E. C. Y. Yan, E. Borguet, K. B. Eisenthal, "Second harmonic generation from the surface of centrosymmetric particles in bulk solution", Chem. Phys. Lett. **259**, 15 (1996).

4. S.-H. Jen, H.-L. Dai, "Probing Molecules Adsorbed at the Surface of Nanometer Colloidal Particles by Optical Second-Harmonic Generation", J. Phys. Chem. B **110**, 23000 (2006).

5. J. I. Dadap, J. Shan, T. F. Heinz, "Theory of optical second-harmonic generation from a sphere of centrosymmetric material: small-particle limit", J. Opt. Soc. Am. B **21**, 1328 (2004).

6. N. Yang, W. E. Angerer, A. G. Yodh, "Angle-Resolved Second-Harmonic Light Scattering from Colloidal Particles", Phys. Rev. Lett. **87**, 103902 (2001).

7. S.-H. Jen, G. Gonella, H.-L. Dai, "The Effect of Particle Size in Second Harmonic Generation from the Surface of Spherical Colloidal Particles. I: Experimental Observations", J. Phys. Chem. A **113**, 4758 (2009).

8. G. Gonella, H.-L. Dai, "Second Harmonic Light Scattering from the Surface of Colloidal Objects: Theory and Applications", Langmuir **30**, 2588−2599 (2014).

9. H. B. de Aguiar, R. Scheu, K. C. Jena, A. G. F. de Beer, S. Roke, "Comparison of scattering and reflection SFG: a question of phase-matching", Phys. Chem. Chem. Phys. **14**, 6826 (2012).

10. B. Schürer, S. Wunderlich, C. Sauerbeck, U. Peschel, W. Peukert, "Probing colloidal interfaces by angle-resolved second harmonic light scattering", Phys. Rev. B **82**, 241404(R) (2010).

11. G. Gonella, H.-L. Dai, "Determination of adsorption geometry on spherical particles from nonlinear Mie theory analysis of surface second harmonic generation", Phys. Rev. B **84**, 121402(R) (2011).

12. B. R. Watson, B. Doughty, T. R. Calhoun, "Energetics at the Surface: Direct Optical Mapping of Core and Surface Electronic Structure in CdSe Quantum Dots Using Broadband Electronic Sum Frequency Generation Microspectroscopy", Nano Lett. **19**, 6157 (2019).

13. J. Wang, X. Wu, Y. He, W. Guo, Q. Zhang, Y. Wang, Z. Wang, "Investigation of the Electronic Structure of CdS Nanoparticles with Sum Frequency Generation and Photoluminescence Spectroscopy", J. Phys. Chem. C **123**, 27712 (2019).

14. G. Olbrechts, E. J. H. Put, K. Clays, A. Persoons, N. Matsuda, "Probing of spatial orientational correlations between chromophores in polymer films by femtosecond hyper-Rayleigh scattering", Chem. Phys. Lett. **253**, 135 (1996).

15. S. Roke, G. Gonella, "Nonlinear Light Scattering and Spectroscopy of Particles and Droplets in Liquids", Ann. Rev. Phys. Chem. **63**, 353 (2012).

16. H. M. Eckenrode, S.-H. Jen, J. Han, A.-G. Yeh, H.-L. Dai, "Adsorption of a Cationic Dye Molecule on Polystyrene Microspheres in Colloids: Effect of Surface Charge and Composition Probed by Second Harmonic Generation", J. Phys. Chem. B **109**, 4646 (2005).

17. L. H. Haber, S. J. J. Kwok, M. Semeraro, K. B. Eisenthal, "Probing the colloidal gold nanoparticle/aqueous interface with second harmonic generation", Chem. Phys. Lett. **507**, 11 (2011).

18. H. Wang, E. C. Y. Yan, Y. Liu, K. B. Eisenthal, "Energetics and Population of Molecules at Microscopic Liquid and Solid Surfaces", J. Phys. Chem. B **102**, 4446 (1998).

19. P.-M. Gassin, S. Bellini, J. Zajac, G. Martin-Gassin, "Adsorbed Dyes onto Nanoparticles: Large Wavelength Dependence in Second Harmonic Scattering", J. Phys. Chem. C **121**, 14566−14571 (2017).

20. Y. El Harfouch, E. Benichou, F. Bertorelle, I. Russier-Antoine, C. Jonin, N. Lascoux, P.-F. Brevet, "Hyper-Rayleigh Scattering from Gold Nanorods", J. Phys. Chem. C **118**, 609 (2014).

21. G. Bachelier, J. Butet, I. Russier-Antoine, C. Jonin, E. Benichou, P.-F. Brevet, "Origin of optical second-harmonic generation in spherical gold nanoparticles: Local surface and nonlocal bulk contributions", Phys. Rev. B **82**, 235403 (2010).

22. J. Butet, G. Bachelier, I. Russier-Antoine, C. Jonin, E. Benichou, P.-F. Brevet, "Interference between Selected Dipoles and Octupoles in the Optical Second-Harmonic Generation from Spherical Gold Nanoparticles", Phys. Rev. Lett. **105**, 077401 (2010).

23. A. Capretti, E. F. Pecora, C. Forestiere, L. Dal Negro, G. Miano, "Size-dependent second-harmonic generation from gold nanoparticles", Phys. Rev. B **89**, 125414 (2014).

24. I. Russier-Antoine, E. Benichou, G. Bachelier, C. Jonin, P. F. Brevet, "Multipolar Contributions of the Second Harmonic Generation from Silver and Gold Nanoparticles", J. Phys. Chem. C **111**, 9044 (2007).

25. R. Dinkel, W. Peukert, B. Braunschweig, "In situ spectroscopy of ligand exchange reactions at the surface of colloidal gold and silver nanoparticles", J. Phys. Condens. Matt. **29**, 133002 (2017).

26. K. B. Eisenthal, "Second Harmonic Spectroscopy of Aqueous Nano- and Microparticle Interfaces", Chem. Rev. **106**, 1462 (2006).

27. M. J. Eilon, T. Mokari, U. Banin, "Surface Exchange Effect on Hyper Rayleigh Scattering in CdSe Nanocrystals", J. Phys. Chem. B **105**, 12726 (2001).

28. M. Jacobsohn, U. Banin, "Size dependence of second harmonic generation in CdSe nanocrystal quantum dots", J. Phys. Chem. B. **104**, 1 (2000).

29. B. S. Santos, G. A. L. Pereira, D. V. Petrov, C. de Mello Donega, "First hyperpolarizability of CdS nanoparticles studied by hyper-Rayleigh scattering", Opt. Commun. **178**, 187 (2000).

30. C. Landes, M. Braun, M. A. El-Sayed, "The effect of surface adsorption on the hyper-Rayleigh scattering of large and small CdSe nanoparticles", Chem. Phys. Lett. **363**, 465 (2002).

31. Y. Zhang, X. Wang, M. Ma, D. Fu, N. Gu, Z. Lu, J. Xu, L. Xu, K. Chen, "Size dependence of second-order optical nonlinearity of CdS nanoparticles studied by hyper-Rayleigh scattering", J. Colloid Interface Sci. **266**, 377 (2003).

32. D. V. Petrov, B. S. Santos, G. A. L. Pereira, C. de Mello Donega, "Size and Band-Gap Dependences of the First Hyperpolarizability of $Cd_xZn_{1-x}S$ Nanocrystals", J. Phys. Chem. B **106**, 5325 (2002).

33. Y. Zhang, X. Wang, D. Fu, J. Cheng, Y. Shen, J. Liu, Z. Lu, "Second-order optical nonlinearity study of CdS nanoparticles via hyper-Rayleigh scattering", J. Phys. Chem. Solids **62**, 903 (2001).

34. R. Tan, D. F. Kelley, A. M. Kelley, "Resonance Hyper-Raman Scattering from CdSe and CdS Nanocrystals", J. Phys. Chem. C **123**, 16400 (2019).

35. S. A. Blanton, R. L. Leheny, M. A. Hines, P. Guyot-Sionnest, "Dielectric Dispersion Measurements of CdSe Nanocrystal Colloids: Observation of a Permanent Dipole Moment", Phys. Rev. Lett. **79**, 865 (1997).

36. R. J. Kortschot, J. van Rijssel, R. J. A. van Dijk-Moes, B. H. Erné, "Equilibrium Structures of PbSe and CdSe Colloidal Quantum Dots Detected by Dielectric Spectroscopy", J. Phys. Chem. C **118**, 7185−7194 (2014).

37. M. Shim, P. Guyot-Sionnest, "Permanent dipole moment and charges in colloidal semiconductor quantum dots", J. Chem. Phys. **111**, 6955 (1999).

38. F. van Mourik, G. Giraud, D. Tonti, M. Chergui, "Linear dichroism of CdSe nanodots: Large anisotropy of the band-gap absorption induced by ground-state dipole moments", Phys. Rev. B **77**, 165303 (2008).

39. L. L. Olenick, J. M. Troiano, N. Smolentsev, P. E. Ohno, S. Roke, F. M. Geiger, "Polycation Interactions with Zwitterionic Phospholipid Monolayers on Oil Nanodroplet Suspensions in Water (D_2O) Probed by Sum Frequency Scattering", J. Phys. Chem. B **122**, 5049 (2018).

40. J.-S. Samsona, R. Scheua, N. Smolentseva, S. W. Rick, S. Roke, "Sum frequency spectroscopy of the hydrophobic nanodroplet/water interface: Absence of hydroxyl ion and dangling OH bond signatures", Chem. Phys. Lett. **615**, 124 (2014).

41. C. J. Ebben, A. P. Ault, M. J. Ruppel, O. S. Ryder, T. H. Bertram, V. H. Grassian, K. A. Prather, F. M. Geiger, "Size-Resolved Sea Spray Aerosol Particles Studied by Vibrational Sum Frequency Generation", J. Phys. Chem. A **117**, 6589−6601 (2013).

42. M. A. Belkin, S. H. Han, X. Wei, Y. R. Shen, "Sum-Frequency Generation in Chiral Liquids near Electronic Resonance", Phys. Rev. Lett. **87**, 113001 (2001).

43. Y. R. Shen, "Surface properties probed by second-harmonic and sum-frequency generation", Nature **337**, 519 (1989).

44. K. B. Eisenthal, "Equilibrium and Dynamic Processes at Interfaces by Second Harmonic and Sum Frequency Generation", Ann. Rev. Phys. Chem. **43**, 627 (1992).

45. P. B. Miranda, Y. R. Shen, "Liquid Interfaces: A Study by Sum-Frequency Vibrational Spectroscopy", J. Phys. Chem. B **103**, 3292 (1999).

46. K. B. Eisenthal, "Liquid Interfaces Probed by Second-Harmonic and Sum-Frequency Spectroscopy", Chem. Rev. **96**, 1343 (1996).

47. G. Lupke, "Characterization of semiconductor interfaces by second-harmonic generation", Surf. Sci. Rep. **35**, 75 (1999).

48. S. Sun, J. Schaefer, E. H. G. Backus, M. Bonn, "How surface-specific is 2nd-order non-linear spectroscopy?", J. Chem. Phys. **151**, 230901 (2019).

49. M. Kauranen, A. Persoons, "Theory of polarization measurements of second-order nonlinear light scattering", J. Chem. Phys. **104**, 3445 (1996).

50. H. B. de Aguiar, A. G. F. de Beer, S. Roke, "The Presence of Ultralow Densities of Nanocrystallites in Amorphous Poly(lactic acid) Microspheres", J. Phys. Chem. B **117**, 8906 (2013).

51. A. N. Bordenyuk, C. Weeraman, A. Yatawara, H. D. Jayathilake, I. Stiopkin, Y. Liu, A. V. Benderskii, "Vibrational Sum Frequency Generation Spectroscopy of Dodecanethiol on Metal Nanoparticles", J. Phys. Chem. C **111**, 8925 (2007).

52. C. Weeraman, A. K. Yatawara, A. N. Bordenyuk, A. V. Benderskii, "Effect of Nanoscale Geometry on Molecular Conformation: Vibrational Sum-Frequency Generation of Alkanethiols on Gold Nanoparticles", J. Am. Chem. Soc. **128**, 14244 (2006).

53. Z. Lu, A. Karakoti, L. Velarde, W. Wang, P. Yang, S. Thevuthasan, H.-f. Wang, "Dissociative Binding of Carboxylic Acid Ligand on Nanoceria Surface in Aqueous Solution: A Joint In Situ Spectroscopic Characterization and First-Principles Study", J. Phys. Chem. C **117**, 24329−24338 (2013).

54. M. T. Frederick, J. L. Achtyl, K. E. Knowles, E. A. Weiss, F. M. Geiger, "Surface-Amplified Ligand Disorder in CdSe Quantum Dots Determined by Electron and Coherent Vibrational Spectroscopies", J. Am. Chem. Soc. **133**, 7476 (2011).

55. B. R. Watson, Y.-Z. Ma, J. F. Cahill, B. Doughty, T. R. Calhoun, "Probing Ligand Removal and Ordering at Quantum Dot Surfaces Using Vibrational Sum Frequency Generation Spectroscopy", J. Colloid Interface Sci. **537**, 389 (2019).

56. B. Doughty, P. Yin, Y.-Z. Ma, "Adsorption, Ordering, and Local Environments of Surfactant-Encapsulated Polyoxometalate Ions Probed at the Air−Water Interface", Langmuir **32**, 8116 (2016).

57. B. Doughty, Y.-Z. Ma, R. W. Shaw, "Probing Interfacial Electronic States in CdSe Quantum Dots Using Second Harmonic Generation Spectroscopy", J. Phys. Chem. C **119**, 2752 (2015).

58. S. Yamaguchi, T. Tahara, "Determining electronic spectra at interfaces by electronic sum frequency generation: One- and two-photon double resonant oxazine 750 at the air/water interface", J. Chem. Phys. **125**, 194711 (2006).

59. L. A. Padilha, J. Fu, D. J. Hagan, E. W. Van Stryland, C. L. Cesar, L. C. Barbosa, C. H. B. Cruz, D. Buso, A. Martucci, "Frequency degenerate and nondegenerate two-photon absorption spectra of semiconductor quantum dots", Phys. Rev. B **75**, 075325 (2007).

60. A. W. Achtstein, et al., "One- and Two-Photon Absorption in CdS Nanodots and Wires: The Role of Dimensionality in the One- and Two-Photon Luminescence Excitation Spectrum", J. Phys. Chem. C **119**, 1260 (2015).

61. M. E. Schmidt, S. A. Blanton, M. A. Hines, P. Guyot-Sionnest, "Size-dependent two-photon excitation spectroscopy of CdSe nanocrystals", Phys. Rev. B **53**, 12629 (1996).

62. C.-K. Lin, J. Lei, Y.-D. Lin, S. H. Lin, "Electronic sum-frequency generation (ESFG) spectroscopy: theoretical formulation of resonances with symmetry-allowed and symmetry-forbidden electronic excited states", Mol. Phys. **115**, 1803 (2017).

63. A. B. Myers, "Molecular electronic spectral broadening in liquids and glasses", Ann. Rev. Phys. Chem. **49**, 267 (1998).

64. A. B. Myers, R. A. Mathies, Resonance Raman Intensities: A Probe of Excited-State Structure and Dynamics. In *Biological Applications of Raman Spectroscopy*, Spiro, T. G., Ed. Wiley: New York, 1987; Vol. 2, pp 1.

65. A. B. Myers, M. O. Trulson, R. A. Mathies, "Quantitation of homogeneous and inhomogeneous broadening mechanisms in *trans*-stilbene using absolute resonance Raman intensities", J. Chem. Phys. **83**, 5000 (1985).

66. K. Gong, D. F. Kelley, A. M. Kelley, "Resonance Raman Excitation Profiles of CdS in Pure CdS and CdSe/CdS Core/Shell Quantum Dots: CdS-Localized Excitons", J. Chem. Phys. **147**, 224702 (2017).

67. J. O. Tollerud, S. T. Cundiff, J. A. Davis, "Revealing and Characterizing Dark Excitons through Coherent Multidimensional Spectroscopy", Phys. Rev. Lett. **117**, 097401 (2016).

68. F. V. A. Camargo, T. Nagahara, S. Feldmann, J. M. Richter, R. H. Friend, G. Cerullo, F. Deschler, "Dark Subgap States in Metal-Halide Perovskites Revealed by Coherent Multidimensional Spectroscopy", J. Am. Chem. Soc. **142**, 777 (2020).

69. G.-H. Deng, Y. Qian, Q. Wei, T. Zhang, Y. Rao, "Interface-Specific Two-Dimensional Electronic Sum Frequency Generation Spectroscopy", J. Phys. Chem. Lett. **11**, 1738 (2020).